Simplified mechanical model to estimate the seismic vulnerability of heritage unreinforced masonry buildings

DIMITRIOS VAMVATSIKOS[1], and STAVROULA J. PANTAZOPOULOU[2]

[1] School of Civil Engineering, National Technical University of Athens, Greece, divamva@central.ntua.gr
[2] Department of Civil and Environmental Engineering, University of Cyprus, Nicosia 1678, Cyprus/ on leave of absence from DUTh, Greece, pantaz@ucy.ac.cy

SUMMARY

Traditional or historic masonry structures occur in large populations throughout the world, particularly in preserved historical city clusters. Being non-engineered and ageing these structures are in urgent need of assessment and seismic repair/rehabilitation. But traditional masonry presents important challenges to computational modeling, owing to complexity of structural system, material inhomogeneity and contact interactions that collectively can only be addressed through detailed 3D nonlinear representation. In this paper, a simple, performance assessment model is developed in order to address the need for preliminary assessment tools for this class of structures. The objective is to be able to rapidly identify buildings that are at higher risk in the event of a significant earthquake, potentially justifying a second round of more detailed evaluation. The proposed model defines the characteristics of a Single Degree of Freedom representation of the building, formulating consistent 3D shape functions to approximate its fundamental mode of vibration considering both in-plane and out-plane wall bending as a result of insufficient diaphragm action. Parametric expressions for the dynamic properties are derived in terms of the important geometric, material, and system characteristics, and are used to express local demand from global estimates. Acceptance criteria are established both in terms of deformation and strength indices to guide retrofit. An application example of the proposed assessment methodology is included, to demonstrate the ability of the model to reproduce the essential features of traditional masonry buildings under seismic action.

KEY WORDS: earthquake; masonry building; simplified model; fragility; static pushover.

1. Introduction

A large number of historical buildings used as traditional family dwellings in the Balkans are almost exclusively of unreinforced masonry (URM) occasionally laced by timber tiers; this structural system is known from ancient times as Opus Craticium. The resistance of URM to lateral loads is primarily imparted by interface friction between interlocking stones, supported due to the overbearing gravity loads. The origin of this construction archetype dates back to pre-Minoan times, continues through classical antiquity and the roman times (Vitruvius 27-23 BC), and has survived in abundance throughout the Balkan region primarily in historical/traditional structures dating to the pre-World War II period. Basic characteristics of this type of construction are (a) the relatively large area ratio of exterior and interior walls which may be either reinforced with timber ties (referred to as tiers) or entirely unreinforced, and (b) the relatively flexible diaphragms.

Post-earthquake reconnaissance reports in S. Europe, record modes of failure in URM buildings typified by diagonal cracking of wall piers, out of plane bending and detachment of piers and dissembling of corner masonry blocks. These are usually owing to the combined absence of diaphragm action, insufficient tying of horizontal to vertical member of the structure and the cumulative implications of poor maintenance and long term phenomena (creep, ageing, corrosion/erosion and soil settlement) [Vintzileou et al. 2007, Simsir et al. 2004, Ceci et al. (2010), Günay and Mosalam (2010)]. Additional problems are associated with the inherent brittleness of unreinforced masonry, occasionally poor workmanship, large self-weight of the structural materials used (including stone roof-tiles) and lack of any design for seismic resistance apart from the empirical traditional practices of the era of construction.

Design and assessment of load-bearing unreinforced masonry structures until recently was not regulated by any established Code of practice. With the introduction of design standards for masonry (EC6, 1989), an outstanding issue regarding high-seismicity regions is the assessment of structural adequacy of existing historical or traditional buildings. From an engineering perspective among existing structures traditional constructions stand out as a special category because: (a) their lateral load resisting system is vague and undefined, (b) they often combine load carrying and secondary components, whereas factors such as ageing, corrosion/depletion of the stone binder and of the timber ties, as well as human intervention, further degrade their seismic resistance.

Due to their heritage significance, rehabilitation of traditional structures is regulated by International Treaties requiring compatibility and reversibility of the intervention [ICOMOS, 1964]. Thus, there is a need for development of uniform methods for seismic assessment and rehabilitation, specifically tailored to the structural system and performance criteria that represent this class of structures. A most difficult issue in this regard is establishing generalized rules for quantifying the seismic vulnerability of traditional structures, firstly due to their great variability of form, but also owing to the different extents of degradation and human intervention they have endured over the years.

On a scale of complexity of application, rapid visual screening and detailed finite element simulation of historical buildings represent the two most remote ends in the spectrum of methods used today for the purposes of seismic assessment of structures. Rapid screening based on visual observation can only assess the condition of the structure and possible damages. Detailed F.E. solutions are fraught with uncertainty with regards to the mechanical behavior of the materials, the extent of damage, and the actual state of interaction that occurs at the interfaces of different materials (e.g. timber and mortar or stones, soil with masonry, etc.). For the needs of seismic assessment (EC8-III 2005), traditional heritage buildings qualify under *knowledge level I* (KL-I): for KL-I, owing to the limited information about material properties and the structural system, the code discourages the use of nonlinear modeling and analysis, but rather, requires the use of simple procedures requiring relatively little computational effort that is comparable to the limited information available. In this case, nonlinear models may be used primarily in order to guide the development, and to corroborate and support the development of simple procedures (see for example the results from a research project PERPETUATE which uses such a nonlinear approach for assessment of cultural heritage buildings with stiff diaphragms, Lagomarsino and Cattari, 2015). However, when shell element modeling is required to model the load bearing walls (this is the case where the building has flexible diaphragms, or poor connectivity between diaphragms and perimeter walls) introducing material nonlinearity in the form of softening and brittleness to represent the unreinforced masonry is practically impossible: the analysis becomes ill-conditioned in the absence of the stabilizing influence of reinforcement, even from the occurrence of the minutest crack (Pantazopoulou 2013).

This paper presents such a simplified procedure intended to be used as a first order assessment tool of the seismic resistance of stone-masonry traditional houses of box-type with flexible diaphragms. The method is formulated using an equivalent SDOF representation of the building's dynamic response. Both demand and supply in the critical locations of the structure needed for evaluation of the acceptance criteria are established in closed-form, in terms of deformation measures, through transformation of global response quantities to local measures. Transformation was based on the shape of fundamental mode of spatial vibration of the structure which was approximated in this study by a 3-dimensional shape function, derived consistently with the boundary conditions of the building. Acceptance criteria are established both in terms of deformation and strength indices. An application example of the proposed assessment methodology is included, to demonstrate the ability of the model to reproduce the essential features of traditional masonry buildings under seismic action.

2. Mechanical Model

2.1. Extending the concepts of Pushover Analysis

The framework of seismic assessment methodologies for steel and concrete structures that has been developed in the past twenty years forms the natural background for development of similar methods geared towards masonry structures. The commonest and most palatable of the available options are nonlinear static approaches where the structure is considered in its fundamental mode of vibration through the Equivalent Single Degree of Freedom (ESDOF) idealization (EC 8-I (2004)). The associated resistance (static pushover) curve is obtained by considering load patterns that follow the height-wise profile of the translational mode.

However, a significant difference between steel or concrete frames and URM structures exists, that complicates direct extension of the established procedures to masonry buildings: Frame structures are mostly lumped systems with stiff diaphragms, whereas URM buildings (at least the types considered in the present paper) have distributed mass and stiffness with typically flexible diaphragms. The consequence of this characteristic is that the fundamental mode of vibration engages a disproportionately low fraction of the building mass, well below the 75% cutoff value for mass participation which is a pre-requisite for the application of the simple ESDOF-based methods.

The alternative option of multimodal pushover analysis (Chopra & Goel 2002) can only be realistically applied with finite element models. In most cases the effort required to obtain dependable results coupled with the degree of uncertainty regarding the actual model properties render this approach beyond the scope of practical assessment of URM structures. Equivalent frame models (Lagomarsino et al. 2013) can be useful in reproducing modes of failure that depend on in-plane strength and stiffness of wall elements, but they are particularly suited to buildings with stiff diaphragms; some types of traditional buildings such as those considered here are particularly susceptible to out-of-plane action owing to flexible diaphragms.

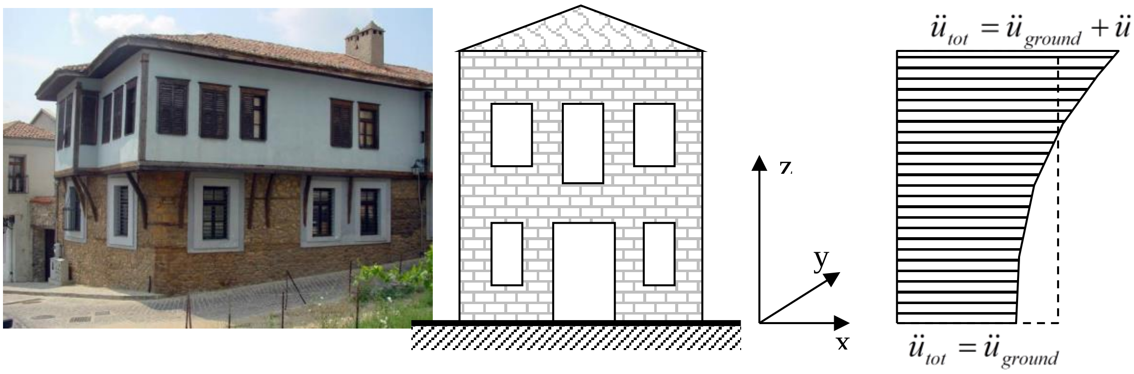

Figure 1. (a) Typical example of timber laced stone-masonry dwelling (b) Idealized Building Model (box) (c) Variation of *total* translational accelerations along building height.

In order to extend the concepts of classical pushover analysis to masonry structures the translational displacement shape is required, $\Phi(x,y,z)$, which is assumed by the structure at the peak of its dynamic response to horizontal ground motion. Through this shape it is also possible to identify and localize the likely points of concentration of anticipated damage from the resulting distribution of deformation implicit in $\Phi(x,y,z)$, while at the same time identifying (a) locations where lack of stiffness may occur and (b) the relative significance of possible mass or stiffness discontinuities.

The shape of lateral translation, $\Phi(x,y,z)$, at the peak of earthquake response, most likely comprises contributions of several modes and mechanisms of deformation, and must necessarily engage a significant fraction of the system's mass during vibration as usually occurs with a random motion such as the ground excitation. In the present study, in order to establish its form, the structure is subjected to a horizontal gravitational field that acts in the direction of the earthquake considered. This approach is based on the observation that pointwise throughout the structure, the earthquake loading $p(x,y,z,t)$ is proportional to the system's mass, $m(x,y,z)$, as follows:

$$p(x,y,z,t) = m(x,y,z) \cdot \ddot{u}_{tot}(x,y,z,t) = w_d(x,y,z) \cdot \ddot{u}_{tot}(x,y,z,t) / g \qquad (1)$$

where, $w_d(x,y,z)$ is the associated value of the weight, $\ddot{u}_{tot}$ the distribution of total acceleration throughout the structure and g the acceleration of gravity; this starts from the value of peak ground acceleration, $\ddot{u}_{ground}$, at ground level, and increases to the total acceleration of the system at the crest of the roof, $\ddot{u}_{tot} = \ddot{u}_{ground} + \ddot{u}$, where u is the relative displacement of the structure with reference to its base support. At peak response, the distribution of total accelerations in Eq. (1) follows a trapezoidal-like distribution, as illustrated in Fig. 1c, starting from the ground acceleration magnitude at the support, to the amplified value at the crest. . From Eq. (1) it follows that the earthquake forces have the same spatial distribution as the mass, naturally increasing with height along with the lateral acceleration. To simplify the calculations, the increase in intensity owing to the height-wise variation of accelerations is neglected in the remainder of this discussion. Instead, a uniform average acceleration pattern along the height of the structure is assumed (shown by a dashed line in Fig. 1c).

The resulting lateral displacement of the structure, $u_d(x,y,z)$, owing to the application of the point-wise value of the weight in the direction of seismic action, has the advantage of satisfying all the essential and natural boundary conditions of the structural vibration problem. For example, the restoring forces that resist the applied gravitational field in the direction of the earthquake satisfy the associated dynamic equilibrium equation since:

$$k \cdot u(x,y,z) = m(x,y,z) \cdot \ddot{u}_{tot}(x,y,z,t) / g \tag{2}$$

and,

$$k \cdot u_d(x,y,z) = w_d(x,y,z) = m(x,y,z) \cdot g \tag{3}$$

It has been shown that the translational shape of vibration, obtained by normalizing the shape of u_d as $\Phi(x,y,z) = u_d(x,y,z)/u_{d,max}$, results in a mass participation factor in the direction of earthquake action, in the range of 90% or more (Pardalopoulos et al. 2013). This procedure has the practical advantage that it enables the use of the familiar features of classical shell analysis software that are used routinely for gravity load analysis of distributed mass systems with the sole input modification over conventional gravity load analysis being the direction of acting gravitational field selected by the user.

Using the translational shape of vibration, the natural frequency of vibration of the system may be approximated with sufficient accuracy using the Rayleigh quotient as follows:

$$\omega^2 = g \cdot \frac{\int_\Omega m \cdot u_d \cdot d\Omega}{\int_\Omega m \cdot u_d^2 \cdot d\Omega} \tag{4}$$

Seismic demands may be determined in terms of total acceleration and displacement of the associated SDOF system (EC8-I (2004) or ASCE-41/06 (2007)). Interestingly the design lateral forces (seismic demand and supply) for load-bearing unreinforced masonry structures, V_{Sd} and V_{Rd}, both depend on the distribution of mass of the URM building (the force demand increases with the system's mass, whereas the frictional resistance at any horizontal plane of sliding increases with the overbearing weight of the structure which is also proportional to the mass (Tastani et al. 2009). For example, higher gravity loads attract a higher seismic base shear (greater mass), but the lateral shear resistance of the walls also increases through enhanced friction. Thus the two terms in the design inequality, $V_{Sd} < V_{Rd}$, interact, to the extent that structural safety may only be assessed for a specific seismic hazard spectrum. In light of the complexity and uncertainties involved in the problem, determination of the performance point for a given ground motion is estimated based on elastic analysis, making allowance for ductility by moderating the force demands and magnifying the displacement demands. To further simplify the process, the important step of the calculation of the shape of translational vibration, $\Phi(x,y,z)$, and the associated characteristics of an equivalent single degree of freedom (ESDOF) approximation of the load-bearing masonry structure are estimated through simplifying assumptions so as to obtain closed form solutions that may provide the basis for easily applicable assessment tools. The derivations are listed in the following sections.

2.2. Estimation of an ESDOF system shape function under lateral translation

Consider a box-shaped rectangular-plan building having external plan dimensions a_{ext}, b_{ext}, with perimeter walls of uniform thickness t and height H (Fig. 2a, b) The corresponding midline dimensions (centerline of the walls) are $a = a_{ext} - t$, $b = b_{ext} - t$. Henceforth, without any loss of generality, the earthquake loading is assumed to act along the *longitudinal* wall of length a, and perpendicular to the *transverse* wall of length b. To approximate the deformed shape assumed by the building at peak lateral translation, the structure is considered under the action of an assumed field of uniform horizontal acceleration acting in the direction of interest. For simplicity the magnitude of the applied acceleration is taken equal to 1g. Through this approach the structure may be analyzed by essentially subjecting it to its own gravity, only taken to act in the direction of the earthquake (Fig. 2b, 2c). The resulting load on the perimeter walls of the mass density ρ_w corresponds to a uniform field force $q(z)$ defined by,

$$q(z) = q = 2\rho_w t(a+b)g \approx W_{tot}/H, \quad z \in [0, H] \tag{5}$$

also approximated in Eq. (5) as the ratio of the total building weight W_{tot} over the building height, to take into account roof and story loads. As illustrated in Fig. 2c, the displaced shape assumed by the structure, in the absence of diaphragms, comprises contributions that result from deformation of walls oriented both parallel (longitudinal) and orthogonal (transverse) to the seismic action. Longitudinal walls are loaded in their plane of action, so that they deform *in-plane*. Transverse walls are loaded normal to their plane of action deforming *out-of-plane*.

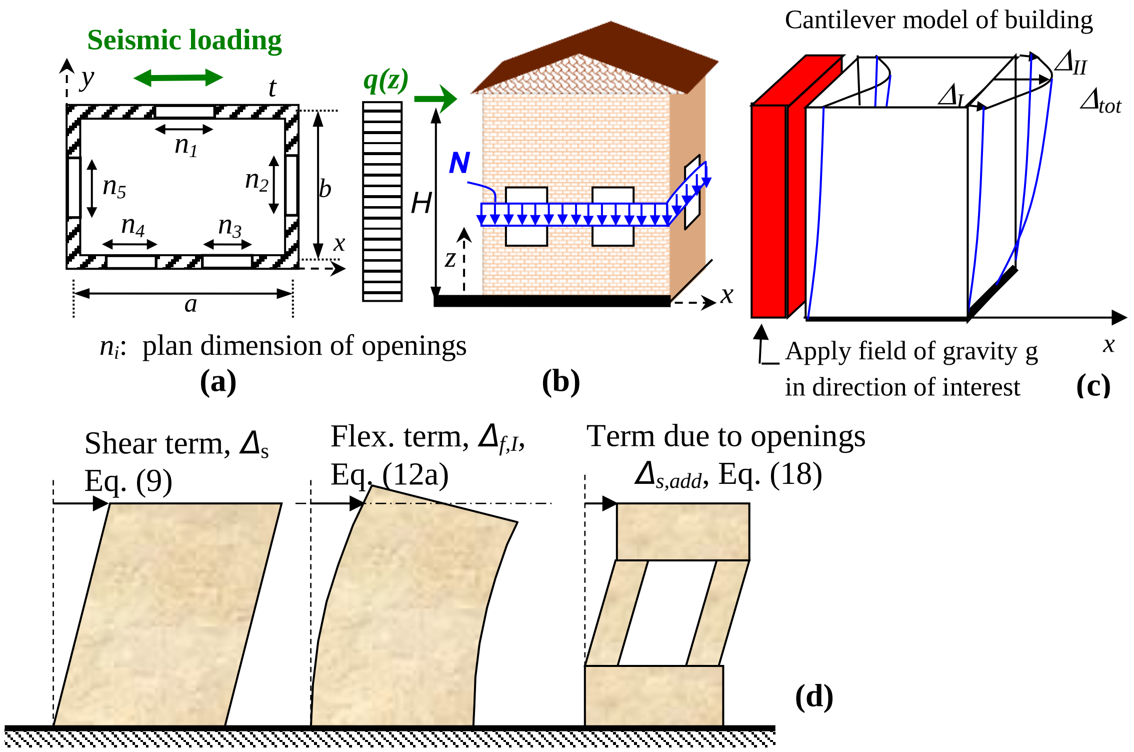

Figure 2. (a) Typical plan of traditional masonry structure, (b) seismic loading, (c) method used to approximate fundamental lateral translational mode of vibration, (d) breakdown of contributions adding to the type-I components of deformation

The in-plane components of deformation are referred to for brevity as *type-I components* (see Fig. 2d). These collectively account for (a) the shear distortion occurring in walls parallel to the load, (b) the flexural drift caused in the structure by the overturning moment of the distributed lateral pressure, and (c) the amplification of lateral distortion at the level of openings due to the increased lateral compliance of the structure at that level. The value of the type-I components only depends upon the vertical coordinate *z*, but not on the in-plan coordinates *x* or *y*.

The out-of-plane components primarily comprise lateral deflections of the transversal walls bending about their weak axis and they are referred to in the remainder as *type-II* components. Their magnitude represents relative displacements of points in the building plan – i.e., within the horizontal plane and it depends on all vertical and horizontal coordinates, *x*, *y* and *z*. The effect of diaphragms becomes a factor on the flexure-only terms of the deformation (i.e., type I and II components), modulating their contribution to the total.

These contributions are combined to define the building's deformation at any point. Of particular interest is the peak lateral translation (usually at some point in the roof), as it will be used to normalize the displacement profile so as to determine a shape, $\Phi(x,y,z)$. The point where the displacement shape after normalization is equal to 1.0 defines the *control node* of the structure, in pushover terms. In symmetric structures this usually occurs at the midcrest of a transverse wall that is bending out of plane (see Figure 2c). Estimating the displacement of the control node for a given level of loading is the goal of the following subsections.

2.2.1 In-Plane Contributions to Lateral Translation: Type I components

The shear and flexural contributions to the Type-I deflection, denoted by Δ_I in Fig. 2c, for walls parallel to the earthquake action, as depicted schematically in Fig. 2d, are evaluated in detail in this section. If the building is seen as a cantilever structure fixed at ground level and free at the roof, having a box-type cross section defined by the building plan, then the walls parallel to the direction of the load serve as the web of the cantilever. At any level *z* from the fixed end, the shear force $V(z)$ and associated shear strain $\gamma_s(z)$ along the building height in the web become:

$$V(z) = \int_z^H q(\zeta)\,\mathrm{d}\zeta = q\left(H - z\right) \tag{6}$$

$$\gamma_s(z) = \frac{V(z)}{G_w A_w} = \frac{q\left(H - z\right)}{A_w G_w} \tag{7}$$

where G_w is the effective shear modulus of the wall. (G_w may be obtained from tests in shear panels as the ascending stiffness of the shear stress – shear strain relationship. It is addressed in detail in Section 2.4; a simplification is to approximate its value as: $G_w \approx 1000\, f_{v,y}$, where $f_{v,y}$ is the shear yield-strength of masonry, usually taken equal to the tensile strength of the material). In the presence of diaphragm action, the wall shear area is taken equal to their plan area $A_w = 2t\cdot(a+b)$; otherwise it is taken equal to the area of the walls parallel to the load, i.e. $A_w = 2t\cdot a$. The resulting horizontal displacement along the loading direction *x* is,

$$d_s(z) = \int_0^z \gamma_s(\zeta)\, d\zeta = \frac{qz\left(2H - z\right)}{2A_w G_w} \tag{8}$$

and the maximum displacement due to shear at the top of the walls is

$$\Delta_s = d_s(H) = \frac{qH^2}{2A_w G_w} \tag{9}$$

Similarly, the moment $M(z)$ and curvature $\phi(z)$ along the height become:

$$M(z) = \int_z^H V(\zeta)\,\mathrm{d}\zeta = \frac{q(H-z)^2}{2} \tag{10}$$

$$\phi(z) = \frac{M(z)}{EI_{plan}} = \frac{q(H-z)^2}{2EI_{plan}} \tag{11}$$

Considering the case where the transverse wall is not allowed to bend locally out of plane, i.e. as if being restrained by an axially rigid diaphragm, the estimated displacement (type I component) along the height of the wall and the corresponding maximum displacement at the top due to flexure would be:

$$d_{f,I}(z) = \int_0^z \phi(\zeta)(z-\zeta)\,\mathrm{d}\zeta = \frac{qz^2}{24EI_{plan}}\left(6H^2 - 4Hz + z^2\right), \tag{12a}$$

$$\Delta_{f,I} = d_{f,I}(H) = \frac{qH^4}{8EI_{plan}} \tag{12b}$$

The *moment* of inertia I_{plan} of the composite plan of the structure (comprising both longitudinal and transverse walls) in the preceding equations is defined by:

$$I_{plan} = \frac{(b+t)(a+t)^3}{12} - \frac{(b-t)(a-t)^3}{12} \tag{13}$$

For a uniform distribution of lateral accelerations along the building height equal to, $S_a=\beta \cdot a_g$, where a_g is the peak ground acceleration (PGA) and β the dynamic amplification coefficient ($\beta \approx 2.5$), the total base shear is, $V_{base}=C_m(W/g)\cdot S_a$; C_m is the mass participation coefficient, taken here as $C_m=0.67$ (Varum 2003, Clough and Penzien 1992, for a flexural cantilever of uniform stiffness and mass, vibrating in the fundamental mode as a result of support lateral acceleration as illustrated in Fig. 1.c). Considering the overbearing weight of the structure, W, and the overturning moment produced by the lateral forces, $M=(2/3)V_{base}H$ (the lever arm is taken $2/3H$ to account for the fact that occasionally there is significant mass at the roof level), the maximum tolerable value of S_a beyond which flexural cracking would occur (horizontal cracks along the building height owing to this type of flexural action) is estimated from:

$$\frac{S_a}{g} \le 1.2 \cdot \frac{\Omega_w}{C_m \cdot H} \cdot \left[\frac{f_{tm}}{W} + \frac{1}{A_w}\right], \text{ where } \Omega_w = \frac{I_{plan}}{(a+t)/2} \tag{14}$$

where f_{tm} is the tensile strength of the horizontal bed joints. Thus, if the acceleration at the top of the structure for a given event exceeds the above limit it may be assumed that the structure has experienced extensive flexural cracking.

The local increase of the shear compliance of the walls at the level of window openings was disregarded in obtaining Δ_s from Eq. (9). Note that the shear force resultant, $V(z)$ only depends on the level of the cross section examined, defined by coordinate z, regardless of the presence of openings. However, the average shear stress, $\tau(z)$, is amplified locally at the level of openings due to the reduced area of the wall supporting the shear force. The local increase in the average shear stress value is:

$$\tau_{add}(z) = \frac{V(z)}{(1-p_o)A_w} - \frac{V(z)}{A_w} = \frac{V(z)}{A_w} \cdot \frac{p_o}{1-p_o} \quad z \in [z_1, z_2] \tag{14}$$

where p_o is the percentage of the wall plan area A_w (including both longitudinal and transverse walls) occupied by the openings and z_1, z_2 are the lower and upper levels of the opening respectively. The corresponding additional shear strain occurring between levels z_1 and z_2 is,

$$\gamma_{s,add}(z) = \frac{V(z)}{A_w G_w} \cdot \frac{p_o}{1-p_o} = \frac{q(H-z)}{A_w G_w} \cdot \frac{p_o}{1-p_o}, \quad z \in [z_1, z_2] \tag{15}$$

which causes an increase in horizontal displacement at every level $z \geq z_1$:

$$d_{s,add}(z) = \int_{z_1}^{z} \gamma_{s,add}(\zeta)\,\mathrm{d}\zeta = \begin{cases} \dfrac{qp_o}{A_w G_w (1-p_o)}(z - z_1)[H - 0.5(z + z_1)], & \text{if } z \in [z_1, z_2] \\ \dfrac{qp_o}{A_w G_w (1-p_o)}(z_2 - z_1)[H - 0.5(z + z_1)], & \text{if } z \in [z_2, H] \end{cases} \tag{16}$$

The added displacement at the top now becomes

$$\Delta_{s,add} = d_{s,add}(H) = \frac{qp_o}{A_w G_w (1-p_o)}(z_2 - z_1)[H - 0.5(z_2 + z_1)] \tag{17}$$

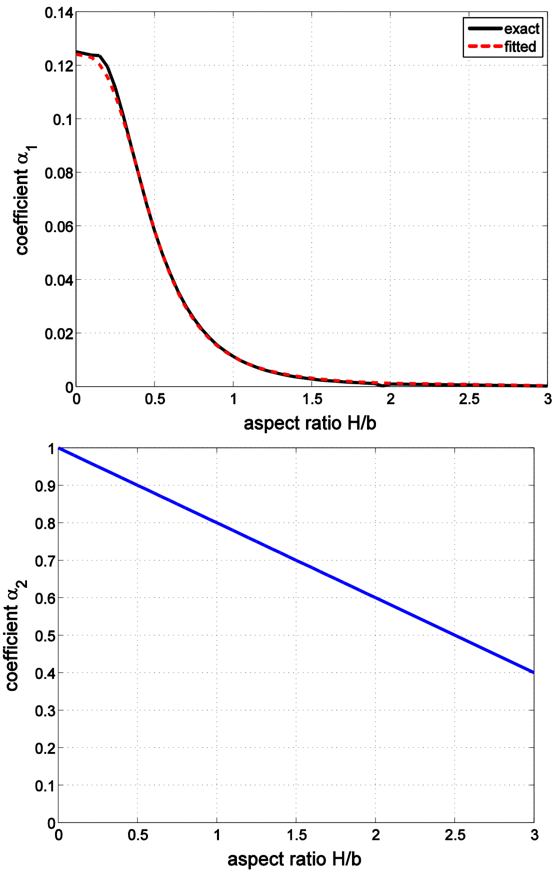

Figure 3: The coefficients used in determining type II flexural deformation at the midcrest of the transverse wall: (a) Variation of a_1 (Eq. (20)), (b) a_2 coefficient (Eq. (21)).

If more than one groups of openings at different levels of z_1, z_2 are to be examined, further $\Delta_{s,add}$ terms will need to be added, one for each group.

2.2.2 Out-of-Plane Contributions to Lateral Translation: Type II Components

The final term needed to complete the deformation analysis is due to the out-of-plane flexure of the transverse walls (type II component). Each transverse wall is modeled by a rectangular plate supported on three out of four edges and uniformly loaded. One edge (the bottom connecting to the foundation) is considered clamped. The other two adjacent edges (where the transverse wall is supported by the longitudinal ones) are partially restrained against rotation about the z axis. If the two partially clamped edges are taken to the limit of simple supports (no rotational restraint), then the analytical solutions by Timoshenko & Woinowsky-Krieger (1987) for the deformation shape due to uniform loading are applicable. By incorporating an empirical factor to take into account the effect of partial clamping, the maximum displacement at the middle of the free edge (midcrest point) under uniform load $q_x = \rho_w g t$ becomes:

$$\Delta_{f,II} = a_1 a_2 \frac{\rho_w g t H^4}{D_{plate}}, \quad \text{where} \quad D_{plate} = \frac{E_w t^3}{12(1-\nu^2)} \tag{18}$$

where a_1, a_2 are coefficients that depend on the aspect ratio H/b of the wall. (To also account for the contribution of roof and storey loads, the unit weight of the walls, $\rho_w g$, may be replaced by, $W_{tot}/H/A_w$.) Coefficient a_1 may be estimated analytically (Timoshenko & Krieger). Nonlinear regression of the results for H/b in [0, 3], which is the range of practical interest, produces the following expression (Fig. 3a):

$$a_1 = 0.0130\left[0.143 + (H/b)^{2.93}\right]^{-1.16} \tag{19}$$

Multiplier a_2 is approximated by a linear function for the same range of aspect ratio values. It is meant to reproduce the effect where a relatively tall wall ($H > b$) will see its midcrest displacement reduced by a greater percentage due to the partial clamping of the vertical edges. Some guidance in choosing its value is provided through analytical solutions [Timoshenko & Krieger (1987)] for the limit case where all three edges are clamped (Fig. 3b):

$$a_2 = 1 - 0.2H/b \tag{20}$$

2.2.3 Effect of Diaphragms in Moderating Differential Displacements

The presence of a diaphragm affects the shape of lateral translation by (a) restraining the (type I) flexural deformation of walls parallel to the seismic action, and (b) reducing the out-of-plane (type II) flexural deformation of transverse walls. Both effects are represented by the empirical reduction factors $\lambda_{f,I}$ and $\lambda_{f,II}$ that define the degree of participation of the (unrestrained) flexural deformations $\Delta_{f,I}$ and $\Delta_{f,II}$ in the total mid-crest displacement.

The bending stiffness of diaphragms relative to the walls is what determines the contribution of the type I flexural deformation to the control-node (midcrest of transverse wall) displacement. Factor $\lambda_{f,II}$ is similarly a direct function of the axial (extensional) stiffness of the diaphragm. The nature of the function connecting the parameters of interest may only be found for specific cases by numerical methods (e.g., FE analysis). Simpler approximations can also be employed, as shown in the Appendix.

2.3 Total Displacement at Mid-Crest and Translational Mode Shape

The peak lateral displacement is expected to occur at the mid-crest of the transverse wall owing to the local amplification effected by the out-of-plane bending of transverse walls unsupported at the crest. Type I displacements prescribe the translation, in the direction of the earthquake, of the walls parallel to the load and thus, of the corner supports of the transverse walls. They comprise the shear deformation of the walls with their openings and the flexural deformation of type I:

$$\Delta_I = \Delta_s + \Sigma\Delta_{s,add} + \lambda_{f,I}\Delta_{f,I} \tag{21}$$

The transverse walls displace out-of-plane (type II deformation) in the direction of the earthquake. The additional deflection at mid-span relative to their corner supports is:

$$\Delta_{II} = \lambda_{f,II}\Delta_{f,II} \tag{22}$$

The total mid-crest displacement becomes:

$$\Delta_{tot} = \Delta_I + \Delta_{II} = \Delta_s + \Sigma\Delta_{s,add} + \lambda_{f,I}\Delta_{f,I} + \lambda_{f,II}\Delta_{f,II} \tag{23}$$

The contribution of each component of deformation to the shape of lateral translation of the entire structure is obtained by normalizing the terms of the above equation with the total displacement at mid-crest, Δ_{tot}.: the resulting normalized displacement pattern at that point assumes the value of 1.0 and thus, the associated point may serve as the control node in determining the performance point on the pushover curve of the structure, from an ESDOF type analysis (ATC 41/06 (2007), EC8-I (2004)). For each mechanism of deformation the following participation factors in the final shape are defined:

$$\delta_I = \frac{\Delta_I}{\Delta_{tot}};\ \delta_{II} = \delta_{f,II} = \frac{\lambda_{f,II}\Delta_{f,II}}{\Delta_{tot}};\ \delta_s = \frac{\Delta_s}{\Delta_{tot}};\ \delta_{s,add} = \frac{\Sigma\Delta_{s,add}}{\Delta_{tot}};\ \delta_{f,I} = \frac{\lambda_{f,I}\Delta_{f,II}}{\Delta_{tot}} \tag{24}$$

so that $\delta_I + \delta_{II} = (\delta_s + \delta_{s,add} + \delta_{f,I}) + \delta_{f,II} = 1$. Each participation factor is used to scale the respective deformation functions in the total translational shape of peak response. For type I components the functional forms are defined from Eqs. (8), (12) and (17), as follows:

$$\begin{aligned}\Phi_I(z) &= \Phi_s(z) + \Phi_{s,add}(z) + \Phi_{f,I}(z)\\ &= \delta_s \frac{z(2H-z)}{H^2} + \delta_{s,add}\frac{\Sigma d_{s,add}(z)}{\Sigma\Delta l_{s,add}} + \delta_{f,I}\frac{z^2}{3H^4}\left(6H^2 - 4Hz + z^2\right)\end{aligned} \tag{25}$$

Note that the last two terms in the right hand side of Eq. (26) are typically dwarfed by the shear deformation of the wall without openings. To further simplify this approximation, these two terms are lumped into the first (shear deformation component) by replacing the participation coefficient δ_s with δ_I in Eq. 25.

$$\Phi_I(z) \approx \delta_I \frac{z(2H-z)}{H^2} \tag{26}$$

While the neglected contributions may be important locally, amplifying point-wise the values of strains and curvatures, they are insignificant in estimating the global ESDOF properties: Typically, δ_s will account for more than 80% of the total type I deformation. Thus, Eq. (27) is ideal for practical estimation of the ESDOF system period and participation factor, whereas Eq. (26) may be used to obtain local deformation demands.

The type II flexural shape of the wall is a complicated function, which is represented only in an approximate way. Thus, at any given distance from the base, *z*, relative outwards displacements across the width of the building, *b*, follow a function that ranges between a sine and a cosine shape, depending on the value of a constant, *c*:

$$\Phi_{f,II}(y) = \frac{\sin(c\pi y/b - p_c) + \sin(p_c)}{1+\sin(p_c)}, \quad \text{where} \quad p_c = (c-1)\pi/2 \tag{27}$$

The significance of this assumption pertains to the degree of clamping at the vertical supports of transverse walls as implied by the lateral deflected shape of the plan of a simple rectangular structure depicted in the mode shapes of Fig. 4(a) or (b). Thus, parameter *c* takes on values between 1 and 2 thereby transforming Eq. (28) from a half-sine shape (appropriate for out-of-plane deflection of a wall pinned at the ends) to a full cosine shape (for a wall with clamped ends) to represent different degrees of fixity along the vertical edges of the transverse wall.

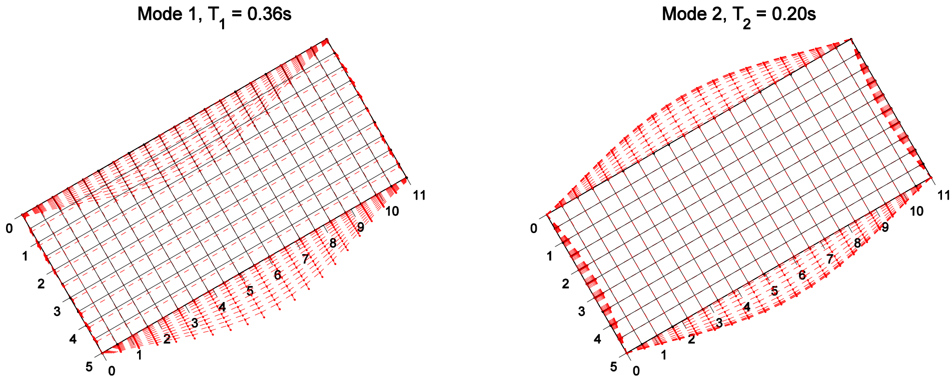

Figure 4. (a), (b) Plan-view of the first two eigenmodes for a rectangular-plan masonry structure with flexible diaphragms (*H* = 6m, *a* = 5m, *b* = 11m, *t* = 0.60m).

The partial clamping is best represented by a value of *c* = 1.5, which is adopted for the local shape in order to define *local* failure criteria. Based on extensive parametric studies with the above expression, there is little to be gained for the global ESDOF system properties by using the more complex expressions associated with this value of *c*. Thus the simpler and analytically more tractable sinusoidal shape of *c* = 1 is preferred instead, when extracting the *global* ESDOF system properties. Variation along the height z is provided by a cubic polynomial that resembles the shape of shear deformation found earlier. Altogether, the type II displacement shape of the transverse wall that determines its additional lateral translation relative to the wall edges (whose displacements are defined by Eq. (26)), becomes:

$$\begin{aligned}\Phi_{II}(y,z) = \Phi_{f,II}(y,z) &= \delta_{II}\frac{z^2(2H-z)}{H^3}\frac{\sin(1.5\pi y/b - 0.25\pi) + \sqrt{2}/2}{1+\sqrt{2}/2} \\ &\cong \delta_{II}\frac{z^2(2H-z)}{H^3}\sin\frac{\pi y}{b}, \qquad y\in[0,b], \quad z\in[0,H]\end{aligned} \tag{28}$$

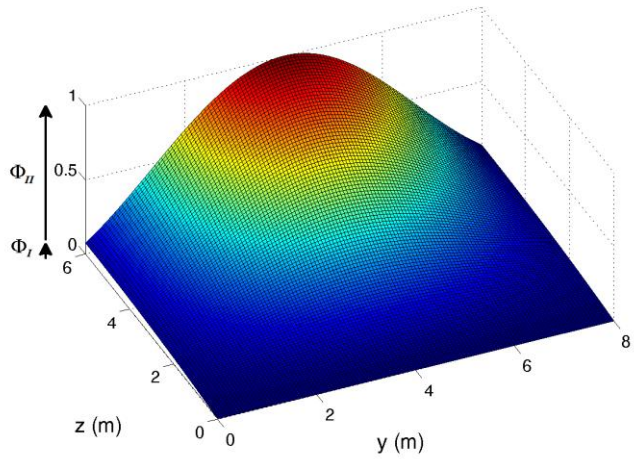

Figure 5. The shape function assumed by Eq. (30) for the total deformation of the transverse wall for H = 6m, a = 8m, b = 8m, t = 0.625m. As shown by the arrows, the Φ_I term determines the displacement at the corners, but Φ_{II} clearly dominates at midcrest.

For the longitudinal walls, only type I deformation is possible, thus only $\Phi_I(z)$ is needed to describe their distribution pattern. For the transverse walls (and story or roof diaphragms, assuming no separation has occurred), both types of deformation are present. Thus, their total shape is obtained from the added contributions of Eq. (27) and (29):

$$\Phi_t(y,z) = \Phi_I(z) + \Phi_{II}(y,z) \tag{29}$$

The total deformation for the any level of seismic loading and for any part of the structure may now be estimated by multiplying the appropriate type I or type I+II shape functions with the corresponding seismic displacement demand Δ_{tot} estimated for the control node (Fig. 5).

2.4 Masonry Material Behavior

The stress-strain behavior of a masonry element under plane stress is idealized as linear up to the point of apparent yielding (Fig. 6a), whereas the length of the plateau depends on the inherent ductility of the blocks and mortar but also on the manner of construction (timber-laced or not). The nominal shear strength of a masonry element, f_v, is estimated as a weighted product of compressive strength of building block strength f_{bc} and joint mortar compressive strength (EC 6, 2005), f_{mc}: $f_v=1.25kf_{bc}^{0.7}f_{mc}^{0.3}$ (stress terms in MPa, with k in the range of 0.35 to 0.55). The range of values of the parameters listed above may vary, but the mean strength is estimated as 0.5MPa with a standard deviation of 0.15MPa. Note that the code recommended values for the shear distortion upon *yielding* of the masonry wall (yielding here is used to identify the onset of friction-sliding behavior along mortar joints after the occurrence of diagonal cracking) is in the range of 0.1% - 0.15%, whereas the shear strain ductility ranges, reaching values as high as 3 in cases of timber laced masonry (GRECO 2012). The design code model for shear strength rides on a Mohr-Coulomb type of idealization of the behavior of stone masonry (Page 1981, Magenes and Calvi 1997, Magenes and Della Fontana, 1998, Milani et al. 2006); according with this concept, the cracking shear strength (used in the remainder as *apparent yielding*), $f_{v,y}$

, of unreinforced masonry is expressed in terms of the inherent stone-binder cohesion, σ_z is the normal compressive stress clamping the potential sliding plane, and μ is the apparent frictional coefficient.

$$f_{v,y} = c_b + \mu \cdot \sigma_z \tag{30}$$

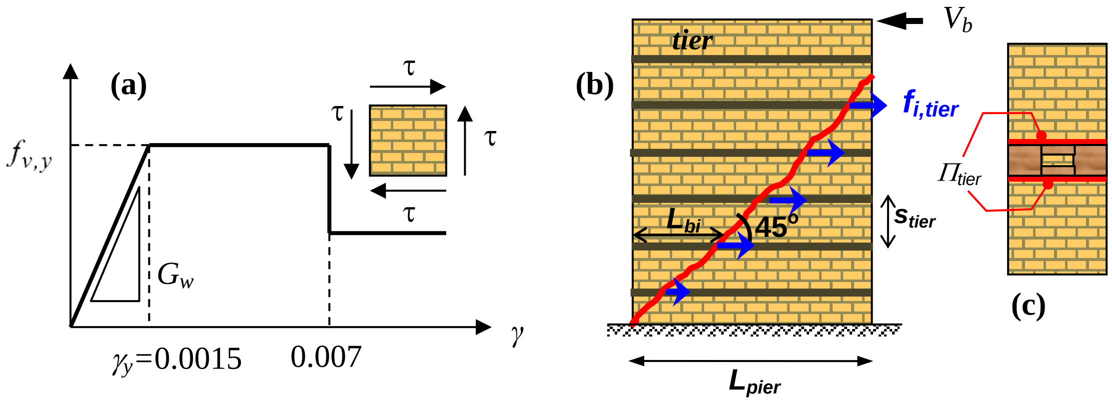

Figure 6. Behavioral Models: (a) Code-recommended resistance curve for masonry wall element, (b) Model illustrating the contribution of timber laces, (c) Tier section

Equation 31 corresponds to the characteristic shear strength of masonry as prescribed by Eq. (3.5) of Eurocode 6 (2005), where the characteristic value for the cohesion is specified in terms of the mortar layer thickness, the type of masonry unit and the type of mortar used for the bed joints, ranging between *0.1* to *0.4 MPa*; the value of μ is taken equal to *0.4* (Tomazevic 2006). An upper limit is set on $f_{v,y}$ by the requirement that it does not exceed the value of $0.065f_b$, where f_b the compressive strength of the typical masonry unit. In applying the code relationship in the present work, the frictional component of shear strength has been neglected, based on the assumption that normal stresses σ_z owing to overbearing loads are very small (in the order of 0.05 to 0.10 MPa). The cohesion c_b may alternatively be taken as the weighted product of tensile (f_{wt}') and compressive (f_{wc}') strengths of the weaker component of the composite masonry (i.e., of the mortar): $c=0.5(f_{wt}' f_{wc}')^{0.5}$ (where f_{wt}' is approximated as $0.1f_{wc}'$); this approach yields commensurate results with those given earlier (conservatively around 0.15 - 0.3 MPa). The contribution of tiers in this strength model is estimated by the total force, V_b, sustained by the number of tier elements (n_{tier}) that intersect a 45° plane of failure after diagonal cracking ($n_{tier}=a/s_{tier}$ where s_{tier} the spacing of tiers in height and a the dimension of the building parallel to the earthquake, Fig. 6(b), (Tastani et al., 2009):

$$V_b = \sum_{i_{tier}=1}^{n_{tier}} A_{tier} f_{i,tier} \tag{31}$$

Parameters A_{tier} and $f_{i,tier}$ are the area and axial stress of the material that acts as tier reinforcement. $f_{i,tier}$ is equal to $u_b \cdot \Pi_{tier} \cdot L_{b,i}$, where u_b is the bond stress at the mortar – timber interface (taken for simplicity equal to the tensile strength of the masonry wall, f_{wt}'), Π_{tier} is the contact perimeter of the cross section of the timber tier element with masonry and $L_{b,i}$ the *minimum* available contact length of tier with the wall, measured to the left or to the right of the diagonal cracking plane. Interface bond is supported by friction due to the overburden pressure, but also due to mechanical interlocking of the transverse ties of the tiers in the masonry (Fig. 6(c)).

2.5 Basic ESDOF system parameters for simple box-type buildings

Deriving the properties of the associated equivalent, or generalized single degree of freedom system (ESDOF) that represents the overall building behavior in spectral coordinates has been the motivating objective for this paper. Thus, the definition of the shape of lateral translation was a necessary intermediate step in the process of estimation of the essential dynamic properties of the ESDOF, namely, the associated mass (mobilized by the response shape), period, excitation coefficient and the corresponding mass participation factor.

The total mass of the system may be found as the sum of the wall masses, the roof mass m_{rf} and any gravity and service loads present on the N_{st} building floors (N_{st} = 1 for a 2-story building). With reference to the building plan of Fig. 2, having a wall mass density ρ_w, and typical floor mass m_{st} (comprising a distributed mass of ρ_{rf} and ρ_{st} per unit area of roof and floor, respectively, and a live load of q), the total system mass becomes:

$$m_{tot} = m_w + m_{rf} + N_{st} m_{st} \tag{32}$$

where, $m_W = 2\rho_W t(a+b)H;\ m_{rf} = \rho_{rf}(a+t)(b+t);\ m_{st} = (\rho_{st} + 0.3q/g)(a+t)(b+t)$.

The generalized mass of the ESDOF is obtained using the translational shape of vibration as follows (Clough and Penzien 1976):

$$\begin{aligned} m &= \int\int \overline{m}(y,z)\left[\Phi_t(y,z)\right]^2 \mathrm{d}z\mathrm{d}y \\ &= 2\int_0^H \rho_w a\, t\Phi_I^2(z)\mathrm{d}z + 2\int_0^H\int_0^b \rho_w t\Phi_{II}^2(y,z)\mathrm{d}y\mathrm{d}z + \sum_{j=1}^{N_{st}} \frac{m_j}{b}\int_0^b \Phi_{II}^2\left(y, \frac{H}{\kappa_j}\right)\mathrm{d}y \end{aligned} \tag{33a}$$

where H/κ_j represents the z coordinate where diaphragm j (or equivalently mass m_j) is located. Thus, by analytic integration:

$$\begin{aligned} m &= \frac{16}{15}\rho_w t H a\,\delta_I^2 + \frac{\rho_w t H b}{105}\left(112\delta_I^2 + \frac{308}{\pi}\delta_I\delta_{II} + 29\delta_{II}^2\right) \\ &+ \sum_{j=1}^{N} m_j \left(\frac{2\kappa_j - 1}{\kappa_j^2}\right)^2 \cdot \left(\delta_I^2 + \frac{4\delta_I\delta_{II}}{\kappa_j\pi} + \frac{\delta_{II}^2}{2\kappa_j^2}\right) \end{aligned} \tag{34b}$$

For example, for a typical two story house, where the mid-story is located at mid-height (at H/2) using $m_1 = m_{st}$, $\kappa_1 = 2$ and $m_2 = m_{rf}$, $\kappa_2 = 1$ simplifies the above expression to:

$$\begin{aligned} m &= \frac{16}{15}\rho_w t H a\,\delta_I^2 + \frac{\rho_w t H b}{105}\left(112\delta_I^2 + \frac{308}{\pi}\delta_I\delta_{II} + 29\delta_{II}^2\right) \\ &+ m_{rf}\left(\delta_I^2 + \frac{4}{\pi}\delta_I\delta_{II} + \frac{1}{2}\delta_{II}^2\right) + m_{st}\frac{9}{16}\left(\delta_I^2 + \frac{2}{\pi}\delta_I\delta_{II} + \frac{1}{8}\delta_{II}^2\right) \end{aligned} \tag{34c}$$

The generalized stiffness of the ESDOF system is estimated following the same concept (Clough and Penzien 1976); the integration is simplified significantly if Poisson effects in plate bending are neglected:

$$K \approx \int_0^H G_w \cdot 2at \cdot \left[\frac{d\Phi_I(z)}{dz}\right]^2 dz + 2\int_0^H\int_0^b E_w \frac{t^3}{12}\left[\frac{\partial^2\Phi_{II}(y,z)}{\partial y^2} + \frac{\partial^2\Phi_{II}(y,z)}{\partial z^2}\right]^2 dy\,dz$$
$$= \frac{8a}{3H} G_w t \delta_I^2 + E_w t^3 \delta_{II}^2 \left(\frac{b}{3H^3} + \frac{\pi^2}{45bH} + \frac{29\pi^4 H}{1260b^3}\right) \tag{34}$$

where $G_w = f_{w,v}^y / \gamma_y$ is the elastic slope of the shear force – shear strain diagram of masonry (units of stress). For example, the average shear stress-strain behavior for common stone masonry walls (without tiers) adopted by Eurocode 8-III (2005) is depicted in Fig. 6(a). The associated period of the system is calculated from:

$$T = 2\pi\sqrt{\frac{m}{K}} \tag{35}$$

The earthquake excitation factor, L_e representing the degree to which the assumed shape of translation is excited by the ground motion is defined by:

$$L_e = \int\int \overline{m}(y,z)\,\Phi_t(y,z)\mathrm{d}z\mathrm{d}y$$
$$= 2\int_0^H \rho_w a\, t\,\Phi_I(z)\mathrm{d}z + 2\int_0^H\int_0^b \rho_w t\,\Phi_{II}(y,z)\mathrm{d}y\mathrm{d}z + \sum_{j=1}^{N_{st}} \frac{m_j}{b}\int_0^b \Phi_{II}\left(y, \frac{H}{\kappa_j}\right)\mathrm{d}y \tag{36}$$
$$= \frac{4}{3}\rho_w t H \delta_I (a+b) + \frac{5}{3\pi}\rho_w t H b \delta_{II} + \sum_{j=1}^{N_{st}} m_j \frac{2\kappa_j - 1}{\kappa_j^2}\left(\delta_I + \frac{2\delta_{II}}{\pi\kappa_j}\right)$$

For the special case of the two story house examined previously:

$$L_e = \frac{4}{3}\rho_w t H \delta_I (a+b) + \frac{5}{3\pi}\rho_w t H b \delta_{II} + m_{rf}\left(\delta_I + \frac{2\delta_{II}}{\pi}\right) + m_{st}\frac{3}{4}\left(\delta_I + \frac{\delta_{II}}{\pi}\right) \tag{37}$$

Furthermore, the effective mass mobilized by the deflected shape, m^* and the associated participation factor Γ may now be estimated as (Clough and Penzien, 1976):

$$\Gamma = \frac{L_e}{m}, \quad m^* = \frac{(L_e)^2}{m} \tag{38}$$

Based on the above calculations, the generalized effective mass for the translational shape considered is found to be in the order of 45-65% depending on the building dimensions; its magnitude underlines the fundamental difference between lumped systems (where the usual value is well over 75% of total mass) from the distributed mass systems such as the one examined herein. The larger the values of a and H are, as compared to b, the higher the effective mass. Since the critical direction of ground excitation for a rectangular building is when it strikes orthogonal to the longer wall, it may be said that in general $b \geq a$, thus, the effective mass will generally be low. Still, the proposed displacement pattern actually represents a much higher percentage of the system's response, as the next significant mode has practically the same period, only the out-of-plane walls bend in opposite directions (as illustrated in Fig. 4). Thus, the proposed shape sufficiently assesses the system behavior and it enables rapid transformation from global to localized seismic demands, and relatively accurate calculations on the seismic vulnerability of a large group of similar buildings. Note that the above expressions can be easily modified to incorporate additional structural components contributing to the mass and stiffness of the structure. For example, interior walls oriented in the direction of the earthquake contribute to mass and stiffness while reducing the unsupported length of transverse walls (their contribution is added on to that of the parallel exterior walls by increasing proportionately the equivalent wall thickness and subdividing the transverse span to $b/2$ in both the mass and stiffness calculations). Interior walls oriented orthogonal to the earthquake contribute to the mass in the same manner as the other transverse walls (i.e., their contribution is accounted for by increasing proportionately the equivalent transverse wall thickness in the mass equations only).

2.6 Performance Evaluation via Nonlinear Static Procedures

The seismic performance of the masonry structure may be evaluated using any nonlinear static procedure, e.g. as specified in EC8-I [2005].The corresponding control node displacement D_{target} is,

$$D_{\text{target}} = \Gamma \cdot C_1 \cdot S_a(T) \cdot \frac{T^2}{4\pi^2} = \Gamma \cdot C_1 \cdot S_d(T) \tag{39}$$

using either the associated demand in spectral acceleration $S_a(T)$ or spectral displacement $S_d(T)$ at period T. C_1 is the inelastic displacement ratio at a strength reduction factor of q (or R), defined as $C_1 = \mu_\mathrm{d}/R$, where μ_d is the ductility demand and

$$R = q = \frac{m^* \cdot S_a(T)}{V_{base,y}} \tag{40}$$

where $V_{base,y}$ is the yield base shear (see following section). Expressions for C_1 are widely available in the literature, e.g., $C_1 = 0.5\,(R^2+1)/R$ for short-periods according to Veletsos and Newmark (Chopra 1995). The displacement demand throughout the structure is obtained from $D_{target} \cdot \Phi_t(x,y,z)$; spatial derivatives of this result provide the local deformation demands (shear distortion angles, relative drift ratios, curvature of walls in out-of-plane bending). In the following sections these values are then compared with the corresponding deformation capacities to assess the potential for failure.

2.7 Capacity curve definition

The response of the structure to a constant horizontal acceleration (pushover load for distributed parameter systems) is idealized by an elastic perfectly plastic capacity curve that terminates at a displacement capacity of Δ_u (blue line in Fig. 7). Thus, only two points of base shear versus roof drift are needed to define the structural behavior, namely nominal yield and ultimate failure. Obviously, several aspects of masonry behaviour are neglected, e.g., the influence of cracking development that introduces a gradual reduction of stiffness in the ascending branch up to yield, and any residual strength that may be available after the ultimate displacement is reached (red curve in Fig. 7). Still, the above assumptions are considered acceptable in view of the considerable uncertainty surrounding masonry.

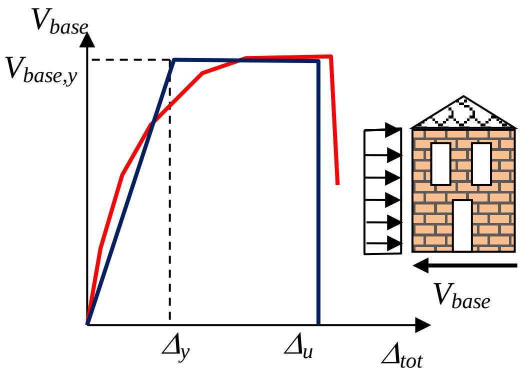

Figure 7. Idealized (blue) and actual (red) pushover curve for masonry structure.

Determination of the performance point is tied to the control node displacement which acts as a multiplication factor on the normalized translational displacement shape of the structure in order to completely determine its local deformation (curvature, strain) profile. This is in essence akin to a displacement-based pushover analysis (e.g., Antoniou and Pinho (2004), Thermou et al. (2007)) in contrast to the typical force-based pushover where the load pattern is constant, with the load factor acting as the multiplier, while the displacement profile changes as the structure is loaded. The adopted approach dispenses with the need for a nonlinear static analysis as everything is determined by the control node displacement and the constant displacement pattern. Thus, in order to estimate the base shear for each given value of the midcrest displacement, all that is needed is the relationship between these two variables, which is implicitly conveyed in the normalized displacement shape.

According to Fig. 6(a) it has been assumed that walls remain elastic up to the nominal yield point. If it is temporarily assumed that this point is associated with yielding of the walls in direct shear, it follows that the shear strength $f_{v,y}$ of the material is attained up to a given height, z, in the structure. If $A_w(z)$ is the wall shear area at this level (comprising the cross sectional area of walls parallel to the plane of action), then the yield shear at this level is,

$$V_y'(z) = f_{v,y} \cdot A_w(z) \tag{42.a}$$

The corresponding value of the horizontal load, q', to cause this level of shear can be found by dividing the above value by $H - z$, i.e., the loaded height of the wall above level z (uniform lateral load) whereas the corresponding yield base shear - assuming that failure occurs at z – is,

$$q' = \frac{V_y'(z)}{H - z} \Rightarrow V'_{base,y} = V_y'(z) \cdot \frac{H}{H - z} \tag{41b}$$

The actual base shear at yield is the minimum value of $V'_{base,y}$, from among all possible failure events occurring at different levels in the structure. Although seemingly tedious, for typical square or rectangular openings, it suffices to check only the values for z at the base of the building ($z = 0$) and at the lowest level of each row of openings.

The corresponding control node displacement Δ'_y due to shear failure at nominal yielding may be found by enforcing nominal deformation limits on the displacement shape determined in the preceding. For example for the walls yielding in shear this is the top displacement for which the displacement shape results in a critical shear strain value equal to the milestone number of 0.0015 listed in the horizontal axis of Fig. 6(a). This establishes the baseline elastic behaviour of the structure. If subsequent checks for “yielding” due to other mechanisms of failure (pertaining to Immediate Occupancy criteria, e.g., cracking of the transverse walls bending out of plane at midspan or at the corners) return a lower control node displacement, Δ_y, then the yield base shear V_{by} is proportionally re-adjusted along this elastic baseline:

$$V_{base,y} = \frac{\Delta_y}{\Delta'_y} \cdot \min_{0 \le z \le H} V'_{base,y}(z) \tag{42}$$

The ultimate displacement is determined by Life Safety or Near Collapse criteria.

Several acceptance criteria and associated limit-states may be recalled in assessing a masonry structure even when response is considered in simple translation as is proposed in the present study. These may be expressed in terms of force or displacement/deformation. The objective in each case is to quantify a limiting value of strain or curvature that may be associated with failure. This limiting value may be related to control node displacement through the deformation shape which enables implementation of the demand-to-capacity check. Four main failure scenarios are presented in the following.

2.7.1 Shear failure of walls

This failure criterion is evaluated by checking the wall shear strain against the limiting strain of γ_{lim}. For this, the shear strain components in type I deformation are considered (being invariable with the transverse coordinate, y) by the first derivative of the corresponding displacement shape. Thus, the shear strain at any level z per meter of control node displacement is

$$\Phi'_{I,s}(z) = \frac{\partial(\Phi_s + \Phi_{s,add})(z)}{\partial z} = 2\delta_s \frac{H-z}{H^2} + \delta_{s,add} \frac{\Sigma \gamma_{s,add}(z)}{\Sigma \Delta_{s,add}} \tag{43}$$

Typically, the additional strain produced by an opening is localized exactly at the level of the opening (although the additional displacement it creates carries through to the top, Eq. (26)). Thus, the sum implied above may contain only one or two terms at each value of z, depending on the openings’ configuration. The minimum value of the midcrest displacement $\Delta_{\gamma,lim}$ corresponding to the attainment of a critical strain value of γ_{lim} can be estimated as:

$$\Delta_{\gamma,lim} = \frac{\gamma_{\lim}}{\max \Phi'_{I,s}(z)} \tag{44}$$

The highest values of shear strain occur at the ground level and at the lowest extremity of each row of openings. Thus, the evaluation of the above equation is much simplified.

2.7.2 Type II (out-of-plane) failure of transverse walls

In response to type-II deformation of the transverse walls, the limited tensile strength of masonry leads to cracking and ultimately to failure. To check for this condition, the curvatures ϕ of the transverse wall are estimated using Eq. (30):

$$\phi_{zz} = \frac{\partial^2 \Phi_t(y,z)}{\partial z^2} = \frac{2\delta_{II}\left(2H-3z\right)}{H^3} \cdot \frac{2\sin\left(1.5\pi y/b - 0.25\pi\right) + \sqrt{2}}{2+\sqrt{2}} - \frac{2\delta_I}{H^2} \quad (45)$$

$$\phi_{yy} = \frac{\partial^2 \Phi_t(y,z)}{\partial y^2} = -\frac{9\pi^2 \delta_{II}}{2(2+\sqrt{2})b^2 H^3} \cdot z^2\left(2H-z\right) \cdot \sin\left(1.5\pi y/b - 0.25\pi\right) \quad (46)$$

$$\phi_{yz} = \phi_{zy} = \frac{\partial^2 \Phi_t(y,z)}{\partial y \partial z} = \frac{3\pi\delta_{II}}{(2+\sqrt{2})bH^3} \cdot z\left(4H-3z\right) \cdot \cos\left(1.5\pi y/b - 0.25\pi\right) \quad (47)$$

The principal values of the curvatures ϕ_1, ϕ_2 may be obtained from standard coordinate transformation:

$$\phi_{1,2} = 0.5(\phi_{yy} + \phi_{zz}) \pm \sqrt{0.25(\phi_{yy} - \phi_{zz})^2 + \phi_{yz}^2} \quad (48)$$

where, ϕ_1 and ϕ_2 identify maximum tension strains either on the interior or the exterior façade of transverse walls. In absolute terms, ϕ_2 attains its maximum at the mid-crest. This is where cracking typically starts on the exterior façade, propagating downwards along the midline and splitting to reach the two lower corners indicating an inverted-Y yield line (Fig. 8a). At the interior, ϕ_1 indicates disjoint cracking at the two upper corners and at the middle of the bottom (Fig. 8a), where the wall attempts to separate from the building.

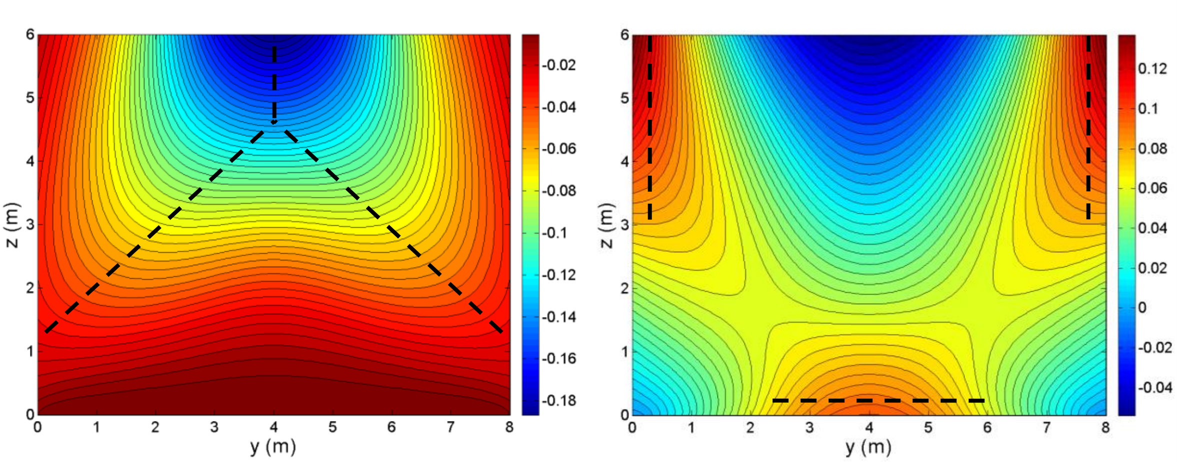

Figure 8. Type-II out-of-plane deformation of transverse wall for H = 5.6m, a = 8m, b = 8m, t = 0.625m: (a) minimum (tension on exterior façade) and (b) maximum (tension on interior façade) principal curvature contours. The ridges (dashed lines) indicate the cracking pattern.

Failure may be defined by the appearance of exterior tension cracks along the top p fraction of the height. For the critical top half, ϕ_{yy} dominates ϕ_2. For a control node displacement of $\Delta_{\varphi,lim}$ the failure condition is written as $\phi_{yy}(y, z)\cdot\Delta_{\varphi,\lim} = \phi_{\lim}$ for $y = b/2$ and $z = (1-p)H$, where $p \in [0,1]$. Solving for $\Delta_{\phi,lim}$, the result is:

$$\Delta_{\phi,lim} = \phi_{lim} \frac{2(2+\sqrt{2})b^2}{9\pi^2(1-p)^2(1+p)\delta_{f,II}} \quad (49)$$

Selecting an appropriate value for the limiting curvature ϕ_{lim} and the percentage p of the cracked path associated with a given performance level are important. For walls without tiers the cracking strain of masonry divided by the distance to the neutral axis may be used, i.e., $\varphi_{cr}=2(0.1f_c^{'}/E_w t)$. In the presence of tiers, the walls possess flexural ductility. Exceeding φ_{cr} may still result in cracking, however, actual failure is now associated with a higher ultimate curvature φ_u. The influence of any openings on the transverse wall can be accounted for by appropriately modifying p. For example, if it is requested that p = 50% of the wall height needs to reach φ_{lim}, then the height of any openings in the top 50% of the transverse wall (especially if close to its midline) can be used to directly reduce the required p.

2.7.3 Type I flexural failure of walls

The type 1 flexural component of deformation may induce failure of the longitudinal walls akin to typical beam bending. Their curvature along the vertical direction, using the more accurate shape proposed, is:

$$\frac{\mathrm{d}^2\Phi_{f,I}(z)}{\mathrm{d}z^2} = 4\delta_{f,I}\frac{(H-z)^2}{H^4} \tag{50}$$

This is maximized at ground level (z=0), and equal to $4\delta_{f,I}/H^2$. Assuming a typical linear distribution of strain along the horizontal dimension (length a) of the longitudinal wall and given a critical strain of ε_{wu}, it is requested that no more than a p percentage of the wall length has exceeded it. This corresponds to a simple limit on the length of the flexural crack that may appear in the long-wall and it is achieved at a curvature value of $\varepsilon_{wu}/(pa)$. As the above estimate of curvature corresponds to a unit control node displacement, by simple analogy the limiting value of mid-crest displacement is:

$$\Delta_{\varepsilon,lim} = \frac{\varepsilon_{wu}/(pa)}{\max[\mathrm{d}^2\Phi_{f,I}(z)/\mathrm{d}z^2]} = \frac{\varepsilon_{wu}H^2}{4pa\delta_{f,I}}. \tag{51}$$

2.7.4 Failure at wall corners

The absolute value of the tension force over a strip of 1m height where the longitudinal wall is pulled apart from the transverse walls is:

$$N_{f,II}(z) = \Delta_{N,t}\cdot E_w I\left.\frac{\partial^3\Phi_t(y,z)}{\partial y^3}\right|_{y=0} = \frac{27\pi^3\delta_{II}\Delta_{N,t}}{8(1+\sqrt{2})b^3H^3}\cdot z^2(2H-z) \tag{52}$$

where I = t^3*(1m)/12 is the moment of inertia of a 1m wide horizontal strip of the longitudinal wall deforming out of plane (type II) and $\Delta_{N,t}$ is the control node displacement when this mode of failure controls. Division by the section area of the strip yields the axial stress that needs to be resisted to prevent cracking, starting from the top of the building and extending down to the value of z where the limiting tensile stress f_{wt} is last exceeded. If the length of such a crack is required to remain less than pH, then, setting $z = H(1 - p)$ and solving for $\Delta_{N,t}$, the value of the associated displacement at the control node may be estimated:

$$\Delta_{N,t} = \frac{32(1+\sqrt{2})b^3}{9E_w t^2\pi^3\delta_{II}(1-p^2)(1-p)}\cdot f_{wt} \tag{53}$$

3 Example application

The preceding sections presented a detailed derivation of the underlying mechanics in support of the proposed simplified method of seismic assessment of simple, box-type URM buildings. An advantage of the procedure is that the end results are given in a closed form expression, enabling automation of the necessary calculations in simple programmable spreadsheets. Application of the methodology is demonstrated here on a simple unreinforced masonry model structure which was tested under simulated ground motions on a shake table by Bothara et al. (2009). The building model was built at a scale of 1:2. The specimen had 0.11m thick masonry walls, a rectangular floor plan of 2.88m x 1.92m and was a two storey structure with a first floor height of 1.34m, a second floor of 1.14m and a roof gable rising by 0.815m.

Masonry prisms were tested to obtain the actual material strengths, as follows: $f_{wc}=16.2$ *MPa*, $\varepsilon_{wc,max}=0.0035$, $E_w=6.1GPa$, $f_{v,y}=0.93MPa$ *(Eq. 33)*, $f_{wt}=0.42$ *MPa*. Bed joint tensile strength is taken as $f_{tm}=0.1MPa$. Shear modulus of the homogenized material G_w, was taken equal to 930MPa (the ratio of an assumed shear strength of 0.93MPa at a cracking shear distortion of 0.1%), whereas the Poisson's ratio was taken $\nu=0.25$. The specific weight γ_w of clay bricks (single brick) was taken 20kN/m^3, whereas for ceramic roof tiles the unit-area weight was taken $\gamma_r=1.5kN/m^2$ including roof trusses and sheathing. Additional masses were added at the gable walls, at the floor level and at the eaves level as follows: (a) for testing in the longitudinal direction added mass per gable was 0.04 ton, 2.1 ton at the floor level and 2.02 ton at the eaves, (b) for testing in the transverse direction, 2.1 ton masses at the floor level and an equal amount at the eaves level respectively. The structure was first tested to a suite of ground motions in the longitudinal direction scaling the ground motion records to pga values in the range of 0.2 – 0.8g; testing was repeated by shaking the structure in the short direction of its plan. In the beginning of the tests recorded fundamental period values were, T_{long} = 0.072 s, T_{short} = 0.102 s. By the end of the tests, due to damage accumulation these values were elongated to T_{long} = 0.11 s, T_{short} = 0.14 s, respectively, i.e., an elongation by a factor of 25%. The analytical model presented in the preceding was used to estimate the structure's response parameters as listed in Table 1. Due to lack of stiff floor panels and connections, no diaphragm action was assumed (i.e., $\lambda_{f,I} = \lambda_{f,II} = 1.0$ in Eq. 24.)

Table 1: Model Parameters for the Bothara et al (2010) test structure for loading along the x-axis (long direction) and the y-axis (short direction). Values are calculated based on the proposed model.

Description	Variable	Reference	x-axis	y-axis
longitudinal wall length	a (m)	Fig.2a	2.77	1.81
transverse wall length	b (m)	Fig.2a	1.81	2.77
roof height	H (m)	Fig.2b	2.48	2.48
wall thickness	t (m)	Fig.2a	0.11	0.11
shear modulus	G_w (MPa)	Fig. 6a	930	930
shear strength	f_v (MPa)	Fig. 6a	0.93	0.93
wall mass	m_w (tn)	Eq. (33)	5.09	5.09
story mass	m_{st} (tn)	Eq. (33)	2.10	2.10
roof mass	m_{rf} (tn)	Eq. (33)	3.19	3.27
total mass	m_{tot} (tn)	Eq. (33)	10.38	10.46
horizontal "gravity" load	q (kN)	Eq. (5)	41.08	41.39
wall total area	A_w (m^2)	Eq. (7)	1.01	1.01
wall box moment of inertia	I_{plan} (m^4)	Eq. (13)	1.16	0.61
resistance of wall plan	Ω_w(m^3)	Eq. (14)	0.8	0.63
wall plate stiffness factor	D_{plate} (kNm)	Eq. (19)	721.70	721.70
Total crest acceleration at flexural cracking ($H=2.48+0.5x0.815$)	S_a $(m\cdot s^{-2})$	Eq. (14)	0.5g	0.38g

shear deformation	Δ_s (mm)	Eq. (9)	0.135	0.135
flexural deformation (Type I)	$\Delta_{f,I}$ (mm)	Eq. (12b)	0.026	0.053
1st floor doors shear deformation	$\Delta_{s,add,1}$ (mm)	Eq. (18)	0.010	0.010
1st floor windows shear deformation	$\Delta_{s,add,2}$ (mm)	Eq. (18)	0.009	0.009
2nd floor windows shear deformation	$\Delta_{s,add,3}$ (mm)	Eq. (18)	0.002	0.002
flexural deformation (Type II)	Δ_{II} (mm)	Eq. (19)	0.35	1.454
type 1 deformation participation	δ_I	Eq. (25)	0.345	0.127
type 2 deformation participation	δ_{II}	Eq. (25)	0.655	0.873
ESDOF generalized mass	m (tn)	Eq. (34c)	3.01	2.50
ESDOF generalized stiffness	K (kN/m)	Eq. (35)	39892	5386.7
ESDOF period	T (sec)	Eq. (36)	0.055	0.135
ESDOF earthquake excitation factor	L_e (tn)	Eq. (38)	4.76	4.01
ESDOF effective mass ratio	m^*/M_{tot}	Eq. (39)	74%	62%
ESDOF participation factor	Γ	Eq. (39)	1.61	1.60

Based on the analysis results tabulated above, the estimated period values were remarkably close to the experimental ones. This is important as the period value controls the spectral demand in practical assessment. Reducing the material moduli to account for cracking to 2/3 of their reference values, produced the same degree of change to the computed periods as reported in the tests. According to test reports, the building did not collapse. Cracking was observed early in the tests and then gradually became more intense and propagated. For an indicative moderate value of mid-crest acceleration equal to $S_a(T_1)$ = 1g in both directions (note that in many of the test runs reported by the authors amplification for the crest point for transverse walls was beyond the 2.5 value assumed by the Type-I EC8-I (2005) Spectrum for the periods of interest), the damage pattern as estimated by the model for two failure conditions is evaluated here, i.e., the shear deformations of the longitudinal walls and the out-of-plane deformation of the transverse wall for each direction of loading.

Due to estimated cracking for the intensity of the applied ground motions, assuming cracked elastic stiffnesses (*2/3* value for E_w and G_w) the analytical values for the elongated periods and the corresponding displacement demands are as follows:

(a) For the longitudinal direction, $T_{long} = 0.055H\ (2/3)^{-1/2} = 0.07s$, $S_d = g\ H\ [0.07 / (2\cdot 3.14)]^2 = 1.22mm$. This value correlates excellently with the reported value of $T_{exp}=0.072\ s$ (*=13.7 Hz*) obtained from longitudinal white noise testing of the structure before cracking. The target displacement was, D_{target} (Eq. 40) = $1.61\ H\ 1.22mm = 2mm$ for $C_1=1$.

(b) Similarly, in the transverse direction, $T_{trans}=0.135\ H\ (2/3)^{-1/2} = 0.165s$. The calculated value correlates adequately with the reported value of $T_{exp}=0.102\ s$ (*=9.8 Hz*) obtained from white noise testing of the structure in the transverse direction before the application of ground motion shaking in that direction. Displacement demand is $S_d=gH[0.165/(2x3.14)]^2 = 6.9mm$, with a target displacement, D_{target} (Eq. 40) = $1.60H6.9mm = 11mm$ for $C_1=1$. Note that these displacement values may be further amplified in the presence of inelastic response (i.e. $C_1>1$).

Nevertheless, it is worth noting here that the top recorded displacement at the crest was near *2mm* for longitudinal shaking, and ranged between *10mm* and *20mm* for various strong shakings in the transverse direction; also, based on the *experimental* evidence, lateral displacement profile had a shape of $\Phi_{long}=\{1,0.7\}$ and $\Phi_{trans}=\{1,0.3\}$, on average, referred to at the centers of floor mass.

To quantify C_1, the behavior factor needs to be estimated in both directions; during the most intense of tests, recorded peak base shear reached *65%* and *55%* of W in the longitudinal and transverse directions, respectively. These numbers are confirmed from the analytical results of Eq. (41) for the total acceleration levels considered, when the effective participating mass is substituted from the results of Table 1: $V_{base}^{long}=m^{*}\cdot S_a = 74\%m_{tot}\cdot 1g = 0.74W$, and $V_{base}^{trans}=m^{*}\cdot S_a=62\%m_{tot}\cdot 1g = 0.62W$; ($W=104\ kN$ based on the m_{tot} value of Table 1).

For the level of shear force, average shear stresses at the base of the wall (Table 2) are well below the strength level of *0.93 MPa*; thus, only localized modes of failure can threaten the integrity of such a box-type structure as seen in the experiments (where only serious damage to the gables was observed).

Table 2: Response Estimates of the Model

Description	Variable	Reference	x-axis	y-axis
Average shear stress at wall base	f_v ,	$V/(2\cdot t\cdot a)$	0.12MPa	0.15MPa
Average shear stress at the lower floor openings ($V/A_{w,red}$)	f_v	Eq. 42.a	0.2 MPa	0.18MPa
Average Shear Distortion of walls // shaking	$\delta_I{}^*D_{target}/H$	δ_I: Table 1	0.0275%	0.05%
Relative displacement at midcrest (relative to the corners);	$\delta_{II}{}^*D_{target}$	δ_{II}: Table 1	1.31mm	9.6mm
Horizontal drift:	$\delta_{II}{}^*D_{target}/(b/2)$		0.037%	0.68%
Crest transverse displacement at vertical splitting through openings†	$\Delta_{\phi,cr}$ (p=50%mm, of which half is in the opening)	Eq. (50)	0.65mm	1.23

†$\phi_{cr} = 2\cdot 0.42MPa/6100MPa/110mm = 1.25\cdot 10^{-6}/mm$.

The above results illustrate that the patterns of anticipated failure would be owing to outwards deflection of the walls orthogonal to the direction of shaking; this is consistent with the experimental reports. Average horizontal drift ratio (relative transverse displacement of the wall midcrest normalized with half the transverse length) is below the *0.1%* limit which represents the cracking limit. However, when localized deformation due to out-of-plane curvature is considered for the walls orthogonal to the direction of shaking, it is seen that mid-crest cracking would propagate down to *25%* of the building height, to the top row of the widows, which would correspond to splitting open the transverse walls down to the mid-height of the structure with no further resistance, at a mid-crest horizontal displacement of *0.65mm* for longitudinal shaking, and *1.23mm* for shaking in the short direction. In light of the fact that total expected displacement for the level of imposed acceleration is *2mm* and *11mm* for the two directions of shaking, it is evident that the corresponding displacement ductility demands were in the order of $\mu_{long}=2mm/0.65mm = 3$, and $\mu_{trans}=11mm/1.23mm = 9$, values that are excessive considering the limited deformation capacity of masonry. However, these levels of deformation are consistent with the observed level of damage which, in the end of the tests was marked with scattering and falling of unsecured tiles, cracking of the gables and extensive cracking of walls in out of plane bending, with vertical cracks propagating through the building's openings.

4 Conclusions

A simplified methodology has been presented for the seismic vulnerability evaluation of box-type traditional buildings with flexible diaphragms. In structures of this category, the budgets available and the degree of complexity in assessing the seismic demands and capacities can be disproportionately complex than the level of knowledge and uncertainty surrounding their condition and properties. The simple model developed in the present paper may serve as a tool for rapid assessment of a single building, but also for collective vulnerability evaluation of clusters of such traditional buildings located in historical settlements. The model reproduces the global vibration characteristics while also employing a local deformation shape to allow estimating typical local failures. For the sake of completeness, the detailed derivation of the underlying mechanics in support of the proposed simplified method was presented in the paper. Of the total number of analytical expressions, those that are needed for seismic assessment of simple, box-type URM buildings are listed in the example case of Table 2. In all cases, no complex structural analysis is needed.

An advantage of the procedure is that the end results are given in closed form expressions, enabling automation of the necessary calculations in simple programmable spreadsheets. A disadvantage is that the assumptions made, in order to simplify the procedures, restrict the applicability of the shape-function used for derivation of the ESDOF properties to simple box-type buildings with rectangular floor plan and flexible floor diaphragms. Although internal dividing walls may be easily incorporated, application of the model to irregular structures is not recommended. In these cases a detailed linear elastic F.E. analysis under a gravitational field in the direction of earthquake action may be a more appropriate way to estimate a shape of lateral translation for the building (Pardalopoulos et al. (2013)). Similarly, if stiff diaphragms are present, further simplifications may be possible such as the equivalent frame method (Lagomarsino 2009).

Application of the procedure to an example URM structure with a rectangular floor plan and flexible diaphragms was included in the paper. A scaled model of the structure had been tested on a shake table to a variety of excitations in the primary and secondary directions of its floor plan. To illustrate the simplicity of calculation possible through the model, the results from essential calculations needed to estimate translational period, displacement demand, base-shear demand, shear-strength estimates and localized capacities are also listed. It is shown that the proposed procedure estimated with very good accuracy the translational periods of the structure in both directions of action, the magnitude of the demands, the pattern of lateral displacement distribution and the tendency for out of plane damage. The requirements for a benchmark presentation of the derivation did not allow for further expansion into the parametric sensitivities of the model; however, such evaluation against many more experimental investigations on URM structures will be pre-requisite to its use for more general fragility curves for this class of structures.

REFERENCES

Antoniou S, Pinho R. Development and verification of a displacement-based adaptive pushover procedure. *Journal of Earthquake Engineering* 2004; **8**(5):643–661.

Bothara JK, Dhakal RP, Mander JB. Seismic performance of an unreinforced masonry building: An experimental Investigation. *Earthquake Engineering and Structural Dynamics* 2010 **39**:45–68.

Ceci A.M., Contento A., Fanale L., Galeota D., Gattulli V., Lepidi M., Potenza F. (2010). “Structural performance of the historic and modern buildings of the University of L’Aquila during the seismic events of April 2009”, Engineering Structures, DOI: 10.1016/j.engstruct.2009.12.023.

CEN. *Eurocode 6: Design of masonry structures, Part 1-1: Common rules for reinforced and*

unreinforced masonry structures. Comité Européen de Normalisation, Brussels, 2005.
CEN. *Eurocode 8: Design of structures for earthquake resistance, Part 1: General rules, seismic actions and rules for buildings.* Comité Européen de Normalisation, Brussels, 2004.
CEN. *Eurocode 8: Design of Structures for Earthquake Resistance, Part 3: Assessment and retrofitting of Buildings*. Comité Européen de Normalisation, Brussels, Brussels, 2005.
Chopra AK, Goel RK. A modal pushover analysis procedure for estimating seismic demands for buildings, *Earthquake Engineering and Structural Dynamics* 2002; **31**:561–582.
Chopra AK. *Dynamics of Structures: Theory and Applications to Earthquake Engineering*. Prentice-Hall: Englewood Cliffs, NJ, 1995.
Clough RW, Penzien J. *Dynamics of Structures.* Mc Graw Hill: New York, 1975, 1992.
GRECO 2012: Greek Code of Interventions Harmonized with EC8-III (2005), European Center on the Prevention and Forecasting of Earthquakes and http://ecpfe.oasp.gr.
Günay S., Mosalam K. Structural Engineering Reconnaissance of the April 6, 2009, Abruzzo, Italy, Earthquake, and Lessons Learned. *PEER Report 2010/105*, 2010.
ICOMOS. International Charter for the Conservation and Restoration of Monuments and Sites, Decisions and Resolutions, Document 1. *IInd International Congress of the Architects and Technicians of Historic Monuments*, Venice, 1964.
URL http://www.international.icomos.org/charters/venice_e.pdf [accessed 10/Nov/2013]
Lagomarsino, S., (2009), "Evaluation and Verification of Out-of-Plane Mechanisms in Existing Masonry, Buildings", *Proc. of the Workshop "Eurocode 8 perspectives from the Italian Standpoint"*, Napoli, 3April 2009
Lagomarsino S., A. Penna, A. Galasco, S. Cattari, (2013). "TREMURI program: An equivalent frame model for the nonlinear seismic analysis of masonry buildings", Engineering Structures, **56**(2013):1787–1799, Elsevier.
Lagomarsino and Cattari, Perpetuate guidelines for seismic performance-based assessment of cultural heritage masonry structures, Bull Earthquake Eng, **13**(1):13–47, 2015
Magenes, G., Della Fontana, A. "Simplified non-linear seismic analysis of masonry buildings", *Proc. Of the British Masonry Society*, No. 8, October 1998, 190-195
Milani G., Lourenço P.B., Tralli A., Homogenised limit analysis of masonry walls, Part I: Failure surfaces, Computers & Structures, 84(3-4):166-180, 2006.
Magenes G, Calvi M. In-plane seismic response of brick masonry walls, Earthq Eng Struct Dyn 26(11):1091-1112, J. Wiley, 1997.
Page A.W. (1981). The biaxial compressive strength of brick masonry. *Proceedings of the Institution of Civil Engineers* **71**(Part 2), 893–906.
Pantazopoulou, S.J. Analysis Methods for Unreinforced Masonry Heritage Structures and Monuments", Electronic Book Commissioned by Organization for Seismic Panning and Protection of Greece, 2013, ecpfe.oasp.gr/en/node/89.
Papadopoulos ML, Pantazopoulou S.J. Simulation for seismic assessment of traditional houses in the historical core of the City of Xanthi before and after non-invasive structural interventions. *Proceedings of the COMPDYN2011 Conference*, Corfu, Greece, 2011.
Pardalopoulos SJ, Pantazopoulou S.J. Seismic assessment of vintage neoclassical buldings through simulation. *Proceedings of the COMPDYN2011 Conference*, Corfu, Greece, 2011.
Simsir CC, Aschheim MA, Abrams DP. Out-of-plane dynamic response of unreinforced masonry bearing walls attached to flexible diaphragms. *Proceedings of the 13th World Conference on Earthquake Engineering*, Vancouver, B.C., 2004.
Tastani S, Papadopoulos M, Pantazopoulou S. Seismic response of traditional masonry buildings: parametric study and evaluation. *Proceedings of the 1st International Conference on Protection of Historical Buildings*, Rome, Italy, 2009.
Thermou G.E., S.J.Pantazopoulou and A.S. Elnashai (2007) "Design methodology for seismic upgrading of substandard RC structures", *J. of Earthquake Engineering*, (Imperial College Press, World Scientific), **11**(4):582 – 606, July 2007.

Timoshenko S, Woinowsky-Krieger S. *Theory of Plates and Shells*. McGraw-Hill: New York, 1987.
Timoshenko S. *Strength of Materials, Part I: Elementary theory and problems, 2nd edition*. D. Von Nostrand Company: NY, 1940.
Tomazevic Miha. *Series on Innovation in structures and construction, Vol. 1:Earthquake-resistant design of masonry buildings*. Imperial College Press: London, UK, 2006.
Varum, H.S.A., Seismic assessment, strengthening and repair of existing buildings, PhD. Thesis, Universidade de Aveiro, (2003), Portugal, 508 pp.
Vintzileou E, Zagkotsis A, Repapis C, Zeris C. Seismic behaviour of the historical structural system of the island of Lefkada, Greece. *Construction and Building Materials* 2007; **21**:225–236.

APPENDIX

The contribution of type I and type II flexural deformations of the walls to the global control node displacement of the system is moderated by two reduction factors, $\lambda_{f,I}$ and $\lambda_{f,II}$. The best approach to estimate them would involve finite element simulations, yet, for the benefit of a simple approach, crude linear approximations may also be employed as follows.

Let $\lambda_{f,I} = f(\theta)$, where θ is the ratio of the bending stiffness of the diaphragm over the bending stiffness of the transverse walls:

$$\theta = \frac{E_c I_{diaph}/a}{E_w I_{wall}/H} \tag{54}$$

where

$$I_{wall} = t_w^3 \cdot b/12, \qquad I_{diaph} = \begin{cases} t_s^3 \cdot b/12, & \text{if diaphragm} = \text{slab} \\ t_b^3 \cdot 2b_w/12, & \text{if diaphragm} = \text{perimeter beams} \end{cases} \tag{55}$$

A concrete slab of t_s thickness is often used as a retrofit measure at each story level, while a perimeter beam of a uniform cross sectional width b_w and depth t_b is a common retrofit measure at the crest. In this context it is assumed that the two perimeter beams at the crest partially restrain the flexural deformation of the longitudinal walls. Note that in this case the transverse wall length, b, affects the resulting values of θ in Eq. (55), while for a slab the term b cancels out. The full restraining effect corresponding to $\lambda_{f,I} = 0$ can be represented by a slab with E_c = 25GPa, E_w = 5GPa, H = 3m, t_w = 0.6m t_s = 0.2m, or a stiffness ratio of θ = 0.2. Then, an appropriate linear function for $\lambda_{f,I}$ is defined as

$$\lambda_{f,I} = \max(1 - 5\theta,\ 0) \tag{56}$$

Factor $\lambda_{f,II}$ is a function of the axial (extensional) stiffness of the diaphragm, k_d. For the purposes of a simple approximation, a linear function is assumed, taking on the value of 1 for k_d = 0 (i.e., when the crest boundary is unrestrained in out-of-plane translation) and 0 when the diaphragm stiffness ratio exceeds a certain critical limit corresponding to the full restraining action of a concrete slab, set here at 60GN/m (which corresponds to full support of the crest boundary against out-of-plane displacement). Then

$$\lambda_{f,II} = \max\left(1 - \frac{k_d}{60\text{GN/m}},\ 0\right) \tag{57}$$

To estimate k_d a slab can be treated like a deep beam of height "*a*" and span "*b*", where *a*, *b* are the plan dimensions of the structure. By solving this as a Timoshenko beam that includes both bending and shear deformations (Timoshenko 1940) we find its midpoint deformation *d* when subjected to a uniform load of $q{\cdot}b$. Then, a measure of the slab's stiffness at the wall midcrest can be obtained as

$$k_{d,slab} = \frac{qb}{d_{mid}} = \frac{384 E_c I_{slab,y}}{b^3\left[1 + 4(1+\nu)(a/b)^2\right]},\ \text{ where } I_{slab,y} = a^3 t_s / 12 \tag{58}$$

For a critical rigid slab assumed of t_s=0.2m, $a = b = 5$m, using $E_c = 25$GPa and $\nu = 0.25$ for concrete we get a value of about 25GN/m. If, instead, a simple perimeter beam is the highest stiffness element restraining the out-of-plane wall bending, a simple Bernoulli beam solution (neglecting shear deformation) can be used to find that two such beams (one on each transverse wall), assumed clamped on both ends, would have a total midpoint stiffness of

$$k_{d,beam} = \frac{qb}{d_{mid}} = \frac{2 \cdot 384 E_c I_{beam,y}}{b^3},\ \text{ where } I_{beam,y} = t^3 t_b / 12\,. \tag{59}$$